
REMAX: Relational Representation for Multi-Agent Exploration

Heechang Ryu
KAIST

Republic of Korea
rhc93@kaist.ac.kr

Hayong Shin
KAIST

Republic of Korea
hyshin@kaist.ac.kr

Jinkyoo Park*
KAIST

Republic of Korea
jinkyoo.park@kaist.ac.kr

Abstract

Training a multi-agent reinforcement learning (MARL) model is generally difficult because there are numerous combinations of complex interactions among agents that induce certain reward signals. Especially when there is a sparse reward signal, the training becomes more difficult. Previous studies have tried to resolve this issue by employing an intrinsic reward, which is a signal specifically designed for inducing the interactions among agents, to boost the MARL model training. However, this approach requires extensive prior knowledge to design an intrinsic reward. To optimize the training of an MARL model, we propose a learning-based exploration strategy to generate the initial states of a game. The proposed method adopts a variational graph autoencoder to represent a state of a game such that (1) the state can be compactly encoded to the latent representation by considering the relationship among agents, and (2) the latent representation can be used as an effective input to the surrogate model predicting the exploration score. The proposed method determines the latent representations that maximize the surrogate model and decodes these representations to generate the initial states from which the MARL model starts training. Empirically, we demonstrate that the generated states improve the training and performance of MARL more than the existing exploration methods.

1 Introduction

Along with deep neural networks, reinforcement learning (RL) has been dramatically improved in the previous decades, and it is exceeding human-level performances in challenging games [23, 29, 30]. The advances in RL and deep learning have naturally generated a significant interest in MARL, as it is expected that the achievements in RL can be extended to solving more complex and large-scale problems that are composed of many agents. In reality, however, the training of an MARL model even for a simple Markov game is generally difficult because the MARL model needs to learn how the interactions among agents and between the agents and the environment induce certain outcomes of the game. Therefore, there is an enormous quantity of possible interactions among agents that the MARL model needs to explore.

Researchers have employed various exploration methods for RL, which can be categorized into three categories: exploration bonus, goal conditioning, and initial state generation methods. The exploration bonus methods provide an intrinsic reward to the agent if the agent visits states that have not been visited. Count-based exploration [2, 25, 31] and curiosity-driven exploration [26, 4, 5] are such types of methods. The goal conditioning methods manipulate the goal of the game to ensure that the agent keeps receiving a reward signal as a result of the sequence of actions it has chosen. By virtually exposing the agent to “success,” it facilitates the RL training [1]. In a similar approach,

*Corresponding author

the difficulty of the goal is increased to ensure that the agent eventually attains a hard-to-achieve goal [13]. Finally, initial state generation methods adjust the initial state distribution to generate the initial states from which an agent can easily complete the task and receive the reward [24, 27, 12, 14]. The common purpose of these three types of exploration methods is to expose the agent to as many rewardable experiences as possible.

While various exploration methods for RL have been proposed, the methods for MARL have been limited. The majority of the exploration methods for MARL provide intrinsic rewards, which are designed to induce actions that can help agents to complete the tasks of a game [3, 16, 34, 15]. However, achieving the design of a good intrinsic reward is generally difficult because it requires prior knowledge of the game. Further, an iterative trial and error approach is often necessitated until a satisfactory result is obtained. Recently, a new exploration method, GENE [17], belonging to the initial state generation for RL and MARL, has been proposed. The method represents the state of a task or game as a latent vector using a variational autoencoder (VAE) [18] and estimates the density of the latent vectors of states using a kernel density estimation (KDE) [10]. By sampling the latent vectors from KDE and decoding them, GENE generates new states that are believed to be novel (exploration) and lead to the good reward (exploitation). The critical limitation of these methods is that they do not take into account the relationships among agents. A simple example illustrating this issue is that the relative locations of n homogeneous agents can be represented as $n!$ different states unless the permutation invariance is employed in the state representation. When focusing on the relative configuration among agents, $n!$ different states can be considered as the same state.

We herein propose an exploration method, called **R**elational representation for **M**ulti-**A**gent **e**xploration (REMAX), to generate novel and rewardable initial states for improving the training of an MARL model. REMAX consists of two parts, state representation and state generation. For state representation, REMAX employs the variational graph autoencoder (VGAE) [19] to extract latent vectors from the states of MARL, such that the latent vectors are effectively used as an input of a surrogate model to predict exploration scores that quantify the balance of exploitation and exploration. In particular, by using a graph encoder based on the graph attention network (GAT) [33] in VGAE, REMAX can effectively represent states by considering the relationships among agents in the states. For state generation, REMAX maximizes the surrogate model to find new latent vectors having high exploration scores and decodes the new latent vectors to generate new initial states. The generated states are then used to train the MARL model. Because VGAE and the surrogate model are trained together in an end-to-end manner, REMAX learns how to generate the initial states that are optimally helpful for boosting MARL training.

2 Related Work

Based on the intuition that the frequent interactions among agents with a reward signal are helpful for training MARL, most of the exploration strategies for MARL employ various intrinsic rewards designed to introduce aggressive interactions among agents. For example, an intrinsic reward is awarded to agents when one agent’s action affects other agents’ behavior or transition [34, 3], which is similar to social influence [16]. The study [15] has proposed a hierarchical method for simultaneously learning policies using different intrinsic rewards for inducing the coordination among agents and proposed to select the policy that maximizes extrinsic returns. However, in general, designing a good intrinsic reward is difficult because it requires prior knowledge of the target game and often requires iterative trial and error approaches until obtaining a satisfactory result.

Recently, GENE [17] has been proposed as a way to generate the initial states to boost the exploration of RL and MARL models. The method is composed of two modules, one for representing a state of the task or game as a latent vector using VAE and another for estimating the density of the latent representation of states using KDE, which are separately trained using the states collected by the RL or MARL models. By sampling the latent vectors from KDE and decoding them, GENE generates new states that are considered to be novel (exploration) and lead to the good reward (exploitation). The method has outperformed the existing methods, such as RND [5], HER [1], Goal GAN [13], Demonstration [24, 27], and RCG [12], in RL, and even the methods extended to multi-agent settings in MARL. In contrast to the existing exploration methods for MARL, the method is easily combined with existing RL and MARL models and does not require prior knowledge of the target task. However, because GENE learns the state representation module (VAE) and the state density estimation module (KDE) separately, the latent representations may not be the best ones for generating novel and

rewardable initial states. We consider GENE as the main comparison method because the method is the most related to REMAX.

3 Background

Multi-Agent Reinforcement Learning. We consider a Markov game [21], which is an extension of the Markov decision process to a game with multiple agents. A Markov game for N agents is defined as follows: $s \in \mathcal{S}$ denotes the global state of the game, and $a_i \in \mathcal{A}_i$ is an action for agent i . The reward for agent i is obtained as a function of the state and joint action as $r_i : \mathcal{S} \times \mathcal{A}_1 \times \dots \times \mathcal{A}_N \mapsto \mathbb{R}$. The state evolves to the next state according to the state transition model $\mathcal{T} : \mathcal{S} \times \mathcal{A}_1 \times \dots \times \mathcal{A}_N \mapsto \mathcal{S}$. The agent i aims to maximize its discounted return $R_i = \sum_{t=0}^T \gamma^t r_i^t$, where $\gamma \in [0, 1]$ is a discount factor. In MARL, each agent learns the policy that maps the state to its action to maximize the accumulated return that is approximated by a Q-function. While the policy can be deterministic $a_i = \mu_i(s)$ or stochastic $a_i \sim \pi_i(\cdot|s)$, one of the basic and widely used models in MARL is the multi-agent deep deterministic policy gradient (MADDPG) [22], which adopts the deterministic policy. MADDPG comprises the individual Q -network and policy network for each agent. In a Markov game, MADDPG lets the Q -network of agent i be trained by minimizing the loss, as follows: $\mathcal{L}(\varphi_i) = \mathbb{E}_{s, \mathbf{a}, r, s' \sim \mathcal{D}}[(Q_i^\mu(s, \mathbf{a}; \varphi_i) - y_i)^2]$, where $\mathbf{a} = (a_1, \dots, a_N)$ represents the actions of all agents, and $y_i = r_i(s, \mathbf{a}) + \gamma Q_i^{\mu'}(s', \mathbf{a}'; \varphi_i)|_{a'_j = \mu'_j(s'; \vartheta'_j)}$. \mathcal{D} is an experience replay buffer that stores (s, \mathbf{a}, r, s') samples. $Q^{\mu'}$ and μ' are target networks for stable learning. The policy network $\mu_i(s; \vartheta_i)$ of agent i is optimized using the gradient computed as $\mathbb{E}_{s, \mathbf{a} \sim \mathcal{D}}[\nabla_{\vartheta_i} Q_i^\mu(s, \mathbf{a}; \varphi_i)] = \mathbb{E}_{s, \mathbf{a} \sim \mathcal{D}}[\nabla_{\vartheta_i} \mu_i(s; \vartheta_i) \nabla_{a_i} Q_i^\mu(s, \mathbf{a}; \varphi_i)|_{a_i = \mu_i(s; \vartheta_i)}]$.

Variational Graph Autoencoder. VGAE is an unsupervised representation learning model for graph-structured data. VGAE consists of a Graph Convolutional Network (GCN) [20] encoder and a simple inner product decoder. The GCN encoder performs posterior inference for latent representations using a node feature matrix and an adjacency matrix of graph-structured data. The decoder performs an inner product between latent variables to reconstruct the adjacency matrix.

Graph Attention Network. GAT is an effective model to process graph-structured data. GAT computes new node embeddings h'_i for the target node i in a graph by aggregating other previous node embeddings h_j from neighboring nodes $\{j \in \mathcal{N}_i\}$ that are connected to the target node i as $h'_i = \sigma(\sum_{j \in \mathcal{N}_i} \alpha_{ij} \mathbf{W}h_j)$. The attention coefficient $\alpha_{ij} = \text{softmax}_j(e_{ij})$, where $e_{ij} = a(\mathbf{W}h_i, \mathbf{W}h_j)$, quantifies the importance of node j to node i in computing h'_i . The attention mechanism effectively differentiates the importance of different nodes in updating the embeddings of the target node. In addition, the attention mechanism can be extended to multi-head attention [32] with K heads.

4 Methods

Figure 1 shows how REMAX runs with a coupled MARL model. First, MARL starts the training by playing a game. When a certain number of states and the associated rewards are collected, REMAX then trains together, in an end-to-end manner, 1) VGAE to represent the state of the game as a latent vector by considering the relationships among agents, and (2) a surrogate model to map the latent vector into the exploration score. Once the learning is finished, REMAX gathers a set of optimized latent vectors by maximizing the continuous surrogate model from randomly generated vectors in the latent space. Finally, REMAX decodes these optimized latent vectors using the trained decoder in the VGAE to generate the initial states of the target game. MARL then starts the next training episodes from the initial states generated by REMAX and collects again new states during the training. The policy training phase by MARL and the state generation phase by REMAX are alternated in training.

4.1 State Representation Using VGAE and Surrogate Model

Encoder of VGAE. We adopt a variant of VGAE [19] to express the states obtained from MARL as latent vectors. Being different from original VGAE using GCN, we use GAT [33] in the encoder part of VGAE because, unlike graph-structured datasets, there is no obvious adjacency matrix in multi-agent settings.

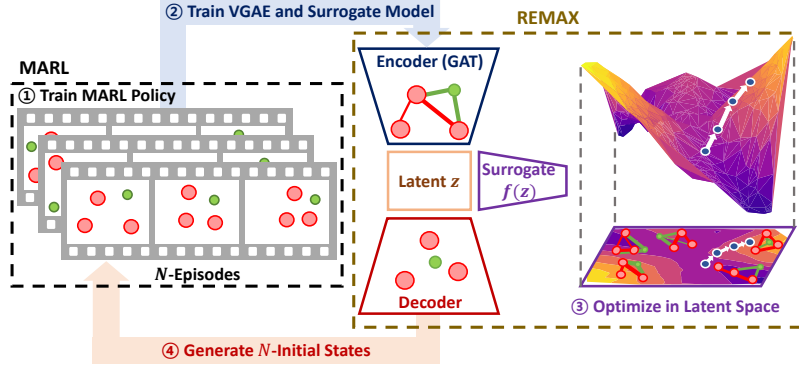


Figure 1: Overview of REMAX.

As an initial step, the GAT encoder reshapes the state $s \in \mathbb{R}^{NF}$ of the game as a set of node features $\mathbf{h} = \{h_1, \dots, h_N\}$ where $h_i \in \mathbb{R}^F$ is the node feature of agent i and N is the number of agents. The importance of node j to node i is then computed as attention coefficients $\alpha_{ij} = \text{softmax}_j(e_{ij}) = \frac{\exp(e_{ij})}{\sum_{m=1}^N \exp(e_{im})}$ where $e_{ij} = \text{LeakyReLU}(\mathbf{v}^T [\mathbf{W}h_i \parallel \mathbf{W}h_j])$. The parameters $\mathbf{W} \in \mathbb{R}^{F' \times F}$ and $\mathbf{v} \in \mathbb{R}^{2F'}$ are optimized during training and shared for all agents. The computed attention coefficients for every state serve as “soft” edges in the graph representing a state of the game, quantifying dynamically the level of interactions among agents.

The updated node feature, called node embedding, for agent i is then computed as a nonlinear transformation of the weighted sum of all node features. Especially, employing multi-head attention, the node embedding $h'_i \in \mathbb{R}^{KF'}$ for agent i can be computed as $h'_i = \|\sum_{k=1}^K \sigma(\sum_{j=1}^N \alpha_{ij}^k \mathbf{W}^k h_j)\|$. For multi-agent settings, as there are various types of interactions among agents, using the multi-head attention is beneficial for extracting the meaningful interactions among agents, especially for non-homogeneous agents.

Once $\mathbf{h}' = \{h'_1, \dots, h'_N\}$ is obtained, it is concatenated as $\|\sum_{i=1}^N h'_i\|$ and transformed to the mean μ and the standard deviation σ for a multivariate Gaussian with a diagonal covariance to sample the latent vector z . In other words, the encoder, the inference model, encodes the states to the latent vectors as $z \sim q_\phi(z|s) = \mathcal{N}(\mu, \sigma^2 \mathbf{I})$ with parameters ϕ .

Decoder of VGAE. For the same reason that there is no obvious adjacency matrix in multi-agent settings, instead of an inner product decoder for reconstructing the adjacency matrix, a general multilayer perceptron (MLP) decoder g_θ is adopted to reconstruct the states. In other words, the decoder, the generative model, decodes the latent vectors to the states using the decoder $p_\theta(s|z)$ or simply $\tilde{s} = g_\theta(z)$ with parameters θ .

Surrogate Model. While VGAE is trained to represent the states as the latent vectors, the surrogate model $f_\psi(z)$ where z is the latent vector in VGAE is simultaneously learned to map z to exploration scores y_s . The exploration score can be flexibly determined. For example, if the MARL model is MADDPG, the Q -networks can be used to compute the score y_s as

$$\frac{1}{N} \sum_{j=1}^N \left[Q_j(s, \mathbf{a}) + \lambda |Q_j(s, \mathbf{a}) - (r_j + \gamma Q'_j(s', \mathbf{a}'))| \right] \quad (1)$$

where the first term, which is an empirical mean of Q [7], quantifies how the corresponding state is valuable for all agents, and thus induces the exploitation. Meanwhile, the second term, which is the empirical mean of TD error [28], quantifies the novelty of the corresponding state, and thus induces the exploration. The hyper-parameter $\lambda \geq 0$ balances between exploitation and exploration. Although λ can be optimally scheduled, we simply use its constant value.

The parameters (θ, ϕ, ψ) for VGAE and the surrogate model are optimized by minimizing the total loss:

$$\mathcal{L}^{\text{total}} = \mathcal{L}^{\text{VGAE}} + \beta \mathcal{L}^{\text{surrogate}} \quad (2)$$

where $\mathcal{L}^{\text{VGAE}}$ is the negative variational lower bound as $-\mathbb{E}_{z \sim q_\phi(z|s)}[\log p_\theta(s|z)] + \text{KL}(q_\phi(z|s) \| p(z))$ where $p(z)$ is a prior as $\mathcal{N}(0, \mathbf{I})$. The $\mathcal{L}^{\text{surrogate}}$ is the mean squared error loss as $\mathbb{E}_{z \sim q_\phi(z|s)}[(f_\psi(z) - y_s)^2]$. The $\beta > 0$ is a hyper-parameter.

4.2 State Generation by Maximizing Surrogate Model

Optimization in Latent Space. After training the surrogate model $f_\psi(z)$ to predict the exploration scores of states based on their latent vectors z , the $f_\psi(z)$ is maximized with respect to z to find new latent vectors having high exploration scores.

First, N_s number of initial latent vectors $\mathbf{z}^0 = \{z_1^0, \dots, z_{N_s}^0\}$ are sampled from $\mathcal{N}(0, \mathbf{I})$. Every vector z_i^0 for $i = 1, \dots, N_s$ is then optimized using the stochastic gradient ascent

$$z_i^{t+1} = z_i^t + \delta(\nabla_{z_i^t} f(z_i^t) + \eta_t) \quad (3)$$

where δ is a step size and η is a Gaussian noise with zero mean and decreasing variance. The noise is injected to prevent the latent vectors from being stuck in local optima over a limited latent space. A set of optimized latent vectors $\mathbf{z}^* = \{z_1^*, \dots, z_{N_s}^*\}$ obtained from \mathbf{z}^0 are then decoded to generate the initial states.

Decoding Latent Vector. Once \mathbf{z}^* is obtained, it is decoded to a set of new states $\mathbf{s}^* = \{s_1^*, \dots, s_{N_s}^*\}$ by using the decoder $\mathbf{s}^* = g_\theta(\mathbf{z}^*)$ of VGAE. MARL then uses \mathbf{s}^* as initial states for the next training episodes.

4.3 Training MARL Policy

After the states corresponding to N_s number of episodes are collected from the training of MARL, REMAX is trained using the states from MARL and generates new initial states for training the MARL policy. To maintain a certain level of exploration, MARL uses the initial states generated from REMAX and the random initial states with a certain probability, such as 0.8:0.2. For every N_s number of training episodes, REMAX is retrained and generates the new initial states for MARL. For training REMAX, the parameters (θ, ϕ, ψ) in REMAX are reinitialized and trained from only newly collected states in the previous training episodes to reflect the evolution of MARL.

5 Experiments

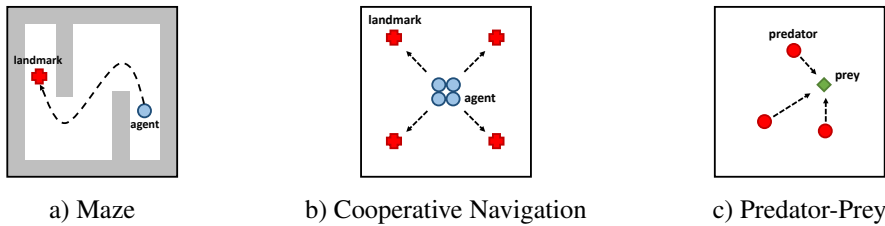


Figure 2: Illustrations of the experimental environments.

Figure 2 shows the environments we use to evaluate the performances of the proposed and comparison methods. The environments are those used in previous studies [17] and those designed to render the reward sparser, which implies that it is more difficult to obtain the reward than in the existing environments. We assume that the agents in the environments have the positions and velocities of all agents as a state, and all the environments impose a penalty on an agent when the agent goes beyond the camera range of the environments. We consider random exploration and GENE as the comparison methods and use MADDPG as an MARL model. Note that any MARL model can be used; however, only MADDPG, one of the most general models, is used as a representative one in this study. All the performance measures are obtained by the trained policies with five different random seeds.

5.1 Maze

The maze is a single-agent environment, shown in Figure 2 (a), which requires an agent (blue circle) to search for the landmark (red cross). When the agent reaches the landmark, it obtains +1 as a reward

and 0 otherwise. Because there is only one agent in this environment, it is not necessary to consider the relationships among agents. Thus, REMAX has VGAE without GAT, which is equivalent to VAE. The structure of REMAX is then similar to that of GENE due to the fact that both use VAE. However, they are different because REMAX uses the surrogate model while GENE uses KDE to evaluate exploration.

Table 1 presents the number of training episodes required for the trained policy to complete the task. Completing a task is defined here as achieving ten consecutive successes starting from the initial states provided by the environment. Thus, a smaller number in the table means that fewer training episodes are needed to train the policy. The latent space dimension denotes the dimension of latent vector z , which is the dimension of the encoding space of VAE. GENE is also reported to have the best performance with one-dimensional latent space. The table shows that REMAX requires fewer episodes than other methods. We believe that the performance gain of REMAX is due to the fact that REMAX trains VAE and surrogate model together in an end-to-end learning, while GENE separately trains VAE and KDE.

The plots in the second row of Figure 3 show how the surrogate model $f_\psi(z)$ and the optimized latent vectors z^* change as the training proceeds, and the plots in the first row show the distribution of generated states s^* represented as green dots. These states are generated by decoding the optimized latent vectors. Figure 4 shows the case where a two-dimensional (2-D) latent space is used for VGAE and the associated 2-D surrogate function. As MARL and REMAX are trained with more samples, as shown in the figures, REMAX tends to generate states near the landmarks because REMAX learns that these states are easily rewardable, and thus, are helpful for MARL training.

Table 1: Number of training episodes in maze.

	Latent space dim.	Episode(x10)
Random	1	640 ± 223
GENE	1	559 ± 255
REMAX	1	456 ± 202
REMAX	2	495 ± 139

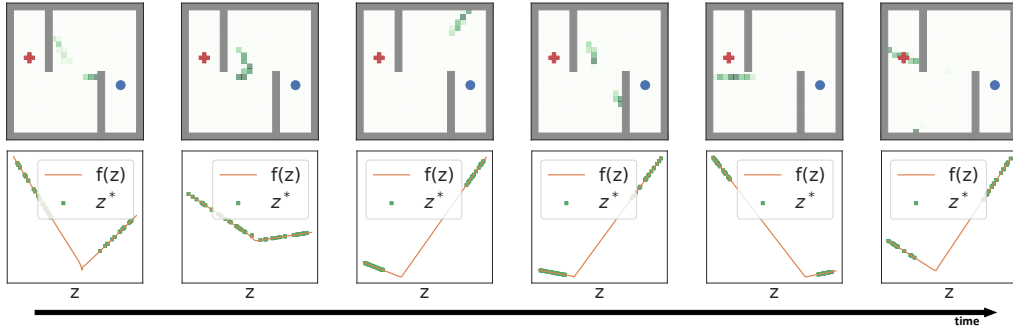


Figure 3: Generated states and surrogate models with one-dimensional latent space in maze.

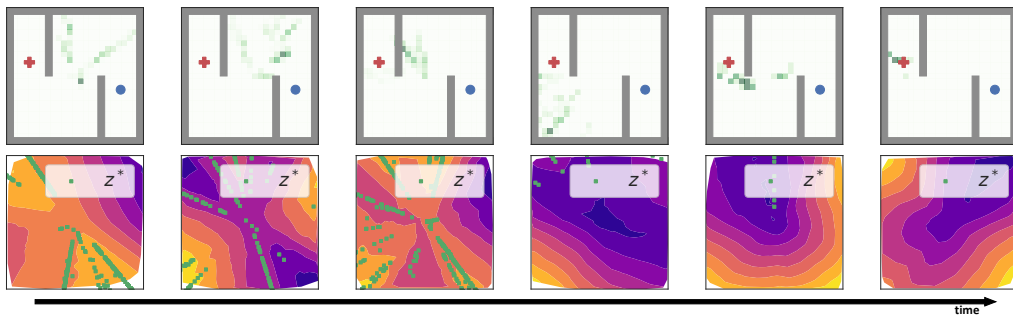


Figure 4: Generated states and surrogate models with two-dimensional latent space in maze.

5.2 Cooperative Navigation

The cooperative navigation is a multi-agent environment, shown in Figure 2 (b), where the homogeneous agents (blue circles) are required to position at the landmarks (red crosses) at four corners. There are as many landmarks as there are agents. Only when every landmark is occupied by one agent, each agent obtains a reward +1 and 0 otherwise. Thus, each agent should be coordinated to occupy a distinct landmark to complete the task.

We conduct ablation experiments to evaluate the synergistic effects of GAT and the surrogate model in REMAX, and the results are summarized in Table 2. The table presents the number of training episodes required for the trained policy to complete the task. In the table, GENE with GAT indicates GENE whose VAE module is replaced with VGAE with GAT encoder. As indicated in the table, compared to GENE, adding GAT to GENE reduces the number of training episodes. We also replace the KDE module in “GENE with GAT” with the surrogate model, and it becomes identical to proposed REMAX. Because REMAX requires a lower number of episodes than the other methods, regardless of the number of agents, the use of both VGAE and the surrogate model is validated to be effective for training the MARL model, especially when the number of agents is large. In addition, the number of episodes for REMAX increases more slowly with the number of agents, which implies that REMAX is the most scalable exploration method for MARL with a large number of agents.

Figure 5 shows the normalized attention coefficients of GAT in the VGAE encoder in REMAX; the thicker the line is, the larger the coefficient. The coefficients between agents increase as multiple

Table 2: Number of training episodes in cooperative navigation.

	Additional architecture				Number of agents		
	VAE	KDE	GAT	Surrogate	2	3	4
Random					583±271	834±168	1178±542
GENE	✓	✓			342±145	632±265	742±540
GENE with GAT	✓	✓	✓		177±64	400±256	454±310
REMAX	✓		✓	✓	161±69	272±80	331±114

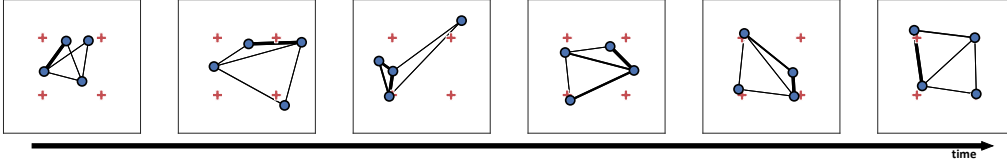


Figure 5: Attention of GAT in REMAX in the cooperative navigation with 4 agents.

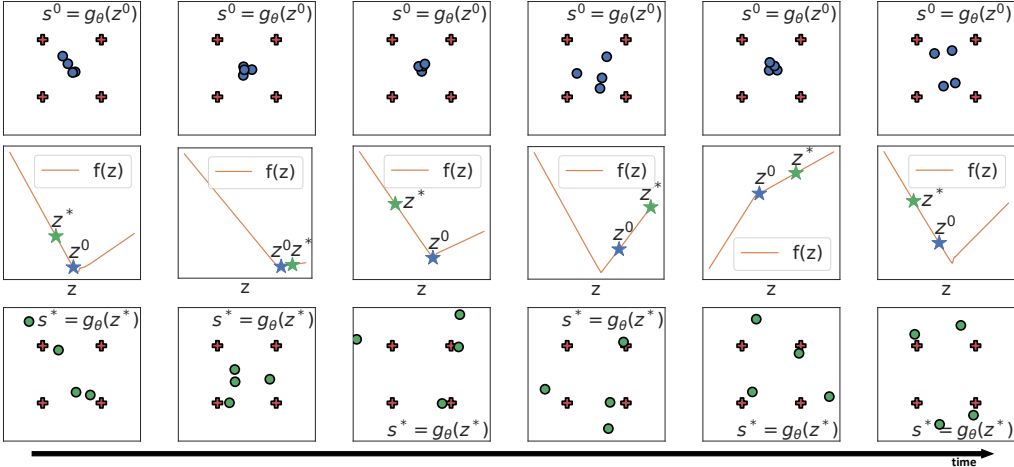


Figure 6: Surrogate models and generated states in the cooperative navigation with 4 agents.

agents approach a common landmark. This trend can be observed in the second figure of Figure 5, which shows the two agents approaching the upper-right landmark, and the fifth figure of Figure 5, which shows the two agents approaching the lower-right landmark.

Figure 6 compares the two states, s^0 decoded from z^0 and s^* decoded from z^* . The figure in the second row shows z^0 and z^* over $f_\psi(z)$. In addition, the figures in the first and third rows show the decoded states from z^0 and z^* by using g_θ . As MARL and REMAX are trained with more samples, as shown in the figure, REMAX tends to generate states near the landmarks.

5.3 Predator-Prey

The predator-prey is a multi-agent environment, shown in Figure 2 (c), where the homogeneous predator agents (red circles) aim to capture the one prey agent (green diamond). Because the prey has faster speed and acceleration than those of the predators, the predators are required to cooperate to capture the prey. In the game, only when two or more predators capture the prey at the same time, each predator obtains a reward +1 and 0 otherwise. Meanwhile, the prey obtains a reward -1 for getting captured. In the predator-prey, we use the GAT encoder with $K = 2$ multi-head attention for REMAX because there are at least two types of relationships, predator-predator and predator-prey.

Table 3 lists the rewards (scores) of the predators trained by each method. After the predators and prey are trained together by each method, the predators are validated for 200 test episodes against the prey trained by random exploration. In the table, REMAX has a higher score than the other methods, which means that the predators trained by REMAX cooperate effectively to capture the prey.

Figure 7 shows the two sets of normalized attention coefficients, α^1 and α^2 , of the GAT encoder with $K = 2$ multi-head attention in REMAX. The two sets of coefficients can quantify the levels of the cooperation among the predators and the competition between the predators and prey, respectively. In the figure, the coefficients (the thickness of the line) increase when two predators approach the prey at the same time. For example, in the fourth figure of Figure 7, two predators are connected with strong attention (upper figure) and, at the same time, both agents are connected strongly with the target prey that they are about to capture together. We identify that the two predators connected by the larger attention coefficients tend to cooperate to capture the prey.

6 Conclusions

We proposed REMAX, an exploration method that generates initial states for accelerating the training of MARL. Empirically, we demonstrated that REMAX generates the states by representing the relationships among agents, and the generated states improve the policy training and performance of MARL more than the existing methods.

Table 3: Scores of predators in predator-prey.

	Random	GENE	REMAX
Score	1.6 ± 0.37	14.3 ± 4.9	18.7 ± 4.6

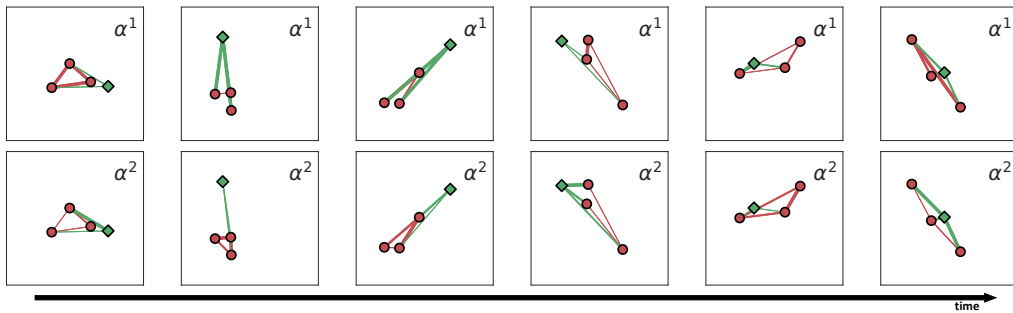


Figure 7: Multi-head attention of GAT in REMAX in predator-prey.

Broader Impact

MARL models have provided a framework for solving large-scale real-world problems in a distributed manner, such as those used in smart grids [9], logistics [35, 6], and distributed vehicles/robots [8, 11]. However, scalability issues and the sparse rewards in these problems have made it challenging for the MARL models to learn to solve the problems. Our work, REMAX, is expected to help the MARL models to learn and solve efficiently large-scale real-world problems by overcoming the scalability issues and sparse rewards. However, the enhanced intelligence generated by MARL could be utilized for unethical purposes. For example, distributed agents with collective intelligence can be used to monitor human beings and to control distributed weapons to harm society. Because the impact of the collective and systemic intelligence employed with a massive number of agents is enormous, these techniques should be carefully executed only for goodwill.

References

- [1] Marcin Andrychowicz, Filip Wolski, Alex Ray, Jonas Schneider, Rachel Fong, Peter Welinder, Bob McGrew, Josh Tobin, OpenAI Pieter Abbeel, and Wojciech Zaremba. Hindsight experience replay. In *Advances in neural information processing systems*, pages 5048–5058, 2017.
- [2] Marc Bellemare, Sriram Srinivasan, Georg Ostrovski, Tom Schaul, David Saxton, and Remi Munos. Unifying count-based exploration and intrinsic motivation. In *Advances in neural information processing systems*, pages 1471–1479, 2016.
- [3] Wendelin Böhmer, Tabish Rashid, and Shimon Whiteson. Exploration with unreliable intrinsic reward in multi-agent reinforcement learning. *arXiv preprint arXiv:1906.02138*, 2019.
- [4] Yuri Burda, Harri Edwards, Deepak Pathak, Amos Storkey, Trevor Darrell, and Alexei A. Efros. Large-scale study of curiosity-driven learning. *International Conference on Learning Representations*, 2019.
- [5] Yuri Burda, Harrison Edwards, Amos Storkey, and Oleg Klimov. Exploration by random network distillation. *International Conference on Learning Representations*, 2019.
- [6] Yongcan Cao, Wenwu Yu, Wei Ren, and Guanrong Chen. An overview of recent progress in the study of distributed multi-agent coordination. *IEEE Transactions on Industrial informatics*, 9(1):427–438, 2013.
- [7] Richard Y Chen, Szymon Sidor, Pieter Abbeel, and John Schulman. UCB exploration via Q-ensembles. *arXiv preprint arXiv:1706.01502*, 2017.
- [8] Peter Corke, Ron Peterson, and Daniela Rus. Networked robots: Flying robot navigation using a sensor net. In *Robotics research. The eleventh international symposium*, pages 234–243. Springer, 2005.
- [9] Emiliano Dall’Anese, Hao Zhu, and Georgios B Giannakis. Distributed optimal power flow for smart microgrids. *IEEE Trans. Smart Grid*, 4(3):1464–1475, 2013.
- [10] Richard A Davis, Keh-Shin Lii, and Dimitris N Politis. Remarks on some nonparametric estimates of a density function. In *Selected Works of Murray Rosenblatt*, pages 95–100. Springer, 2011.
- [11] J Alexander Fax and Richard M Murray. Information flow and cooperative control of vehicle formations. *IEEE transactions on automatic control*, 49(9):1465–1476, 2004.
- [12] Carlos Florensa, David Held, Markus Wulfmeier, Michael Zhang, and Pieter Abbeel. Reverse curriculum generation for reinforcement learning. In *Proceedings of the 1st Annual Conference on Robot Learning*, volume 78 of *Proceedings of Machine Learning Research*, pages 482–495. PMLR, 2017.
- [13] Carlos Florensa, David Held, Xinyang Geng, and Pieter Abbeel. Automatic goal generation for reinforcement learning agents. In *Proceedings of the 35th International Conference on Machine Learning*, volume 80 of *Proceedings of Machine Learning Research*, pages 1515–1528. PMLR, 2018.

- [14] Anirudh Goyal, Philemon Brakel, William Fedus, Soumye Singhal, Timothy Lillicrap, Sergey Levine, Hugo Larochelle, and Yoshua Bengio. Recall traces: Backtracking models for efficient reinforcement learning. *International Conference on Learning Representations*, 2019.
- [15] Shariq Iqbal and Fei Sha. Coordinated exploration via intrinsic rewards for multi-agent reinforcement learning. *arXiv preprint arXiv:1905.12127*, 2019.
- [16] Natasha Jaques, Angeliki Lazaridou, Edward Hughes, Caglar Gulcehre, Pedro Ortega, Dj Strouse, Joel Z. Leibo, and Nando De Freitas. Social influence as intrinsic motivation for multi-agent deep reinforcement learning. In *Proceedings of the 36th International Conference on Machine Learning*, volume 97 of *Proceedings of Machine Learning Research*, pages 3040–3049. PMLR, 2019.
- [17] Jiechuan Jiang and Zongqing Lu. Generative exploration and exploitation. In *Thirty-Fourth AAAI conference on artificial intelligence*, 2020.
- [18] Diederik P Kingma and Max Welling. Auto-encoding variational bayes. *International Conference on Learning Representations*, 2014.
- [19] Thomas N Kipf and Max Welling. Variational graph auto-encoders. *NIPS Workshop on Bayesian Deep Learning*, 2016.
- [20] Thomas N Kipf and Max Welling. Semi-supervised classification with graph convolutional networks. *International Conference on Learning Representations*, 2017.
- [21] Michael L Littman. Markov games as a framework for multi-agent reinforcement learning. In *Machine learning proceedings 1994*, pages 157–163. Elsevier, 1994.
- [22] Ryan Lowe, Yi I Wu, Aviv Tamar, Jean Harb, OpenAI Pieter Abbeel, and Igor Mordatch. Multi-agent actor-critic for mixed cooperative-competitive environments. In *Advances in neural information processing systems*, pages 6379–6390, 2017.
- [23] Volodymyr Mnih, Koray Kavukcuoglu, David Silver, Andrei A Rusu, Joel Veness, Marc G Bellemare, Alex Graves, Martin Riedmiller, Andreas K Fidjeland, Georg Ostrovski, et al. Human-level control through deep reinforcement learning. *Nature*, 518(7540):529, 2015.
- [24] Ashvin Nair, Bob McGrew, Marcin Andrychowicz, Wojciech Zaremba, and Pieter Abbeel. Overcoming exploration in reinforcement learning with demonstrations. In *2018 IEEE International Conference on Robotics and Automation (ICRA)*, pages 6292–6299. IEEE, 2018.
- [25] Georg Ostrovski, Marc G Bellemare, Aäron van den Oord, and Rémi Munos. Count-based exploration with neural density models. In *Proceedings of the 34th International Conference on Machine Learning-Volume 70*, pages 2721–2730. JMLR. org, 2017.
- [26] Deepak Pathak, Pulkit Agrawal, Alexei A Efros, and Trevor Darrell. Curiosity-driven exploration by self-supervised prediction. In *Proceedings of the IEEE Conference on Computer Vision and Pattern Recognition Workshops*, pages 16–17, 2017.
- [27] Cinjon Resnick, Roberta Raileanu, Sanyam Kapoor, Alexander Peysakhovich, Kyunghyun Cho, and Joan Bruna. Backplay: " man muss immer umkehren". *arXiv preprint arXiv:1807.06919*, 2018.
- [28] Tom Schaul, John Quan, Ioannis Antonoglou, and David Silver. Prioritized experience replay. *International Conference on Learning Representations*, 2016.
- [29] David Silver, Aja Huang, Chris J Maddison, Arthur Guez, Laurent Sifre, George Van Den Driessche, Julian Schrittwieser, Ioannis Antonoglou, Veda Panneershelvam, Marc Lanctot, et al. Mastering the game of go with deep neural networks and tree search. *Nature*, 529(7587):484, 2016.
- [30] David Silver, Julian Schrittwieser, Karen Simonyan, Ioannis Antonoglou, Aja Huang, Arthur Guez, Thomas Hubert, Lucas Baker, Matthew Lai, Adrian Bolton, et al. Mastering the game of go without human knowledge. *Nature*, 550(7676):354, 2017.

- [31] Haoran Tang, Rein Houthooft, Davis Foote, Adam Stooke, OpenAI Xi Chen, Yan Duan, John Schulman, Filip DeTurck, and Pieter Abbeel. #Exploration: A study of count-based exploration for deep reinforcement learning. In *Advances in neural information processing systems*, pages 2753–2762, 2017.
- [32] Ashish Vaswani, Noam Shazeer, Niki Parmar, Jakob Uszkoreit, Llion Jones, Aidan N Gomez, Łukasz Kaiser, and Illia Polosukhin. Attention is all you need. In *Advances in neural information processing systems*, pages 5998–6008, 2017.
- [33] Petar Veličković, Guillem Cucurull, Arantxa Casanova, Adriana Romero, Pietro Liò, and Yoshua Bengio. Graph attention networks. *International Conference on Learning Representations*, 2018.
- [34] Tonghan Wang, Jianhao Wang, Yi Wu, and Chongjie Zhang. Influence-based multi-agent exploration. *International Conference on Learning Representations*, 2020.
- [35] Wang Ying and Sang Dayong. Multi-agent framework for third party logistics in e-commerce. *Expert Systems with Applications*, 29(2):431–436, 2005.

Supplementary Material

Surrogate Models and Generated States in Predator-Prey

Figure 8 shows one of the decoded states s^0 from initial latent vectors z^0 in the first row, $f_\psi(z)$ in the second row, and the generated state s^* in the third row after z^* is optimized from the z^0 for the first row. In the second row, the blue and green stars in the figure represent the z^0 for the first row and the z^* for the third row, respectively. The predators in the generated states s^* are more likely to capture the prey than the predators in the states s^0 . In the second figure in Figure 8, the predators in s^* tend to surround the prey more than the predators in s^0 . In the third, fourth, and fifth figures in Figure 8, the predators in s^* tend to be closer to the prey than the predators in s^0 .

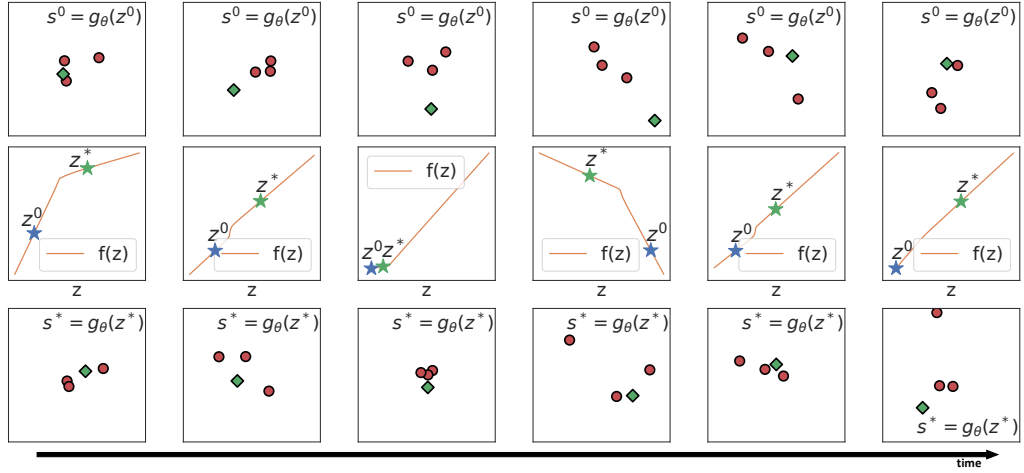


Figure 8: Surrogate models and generated states in predator-prey.

Hyper-parameters for Experiments

The hyper-parameters of REMAX with MADDPG used in each environment are summarized in Table 4. In the table, F includes 2 for x-y position and 2 for x-y velocity in the state of the environments. The maze has the agent within $[0, 1.5]^2$. The positions of agent and landmark, P_a and P_l , in the maze are $(1.25, 0.6)$ and $(0.25, 0.9)$. The cooperative navigation has the agents within $[0, 1]^2$. The agents and landmarks in the cooperative navigation are at the center and at four corners, respectively. In the environments, the landmark is considered to be occupied if $\|P_a - P_l\| < 0.1$. The predator-prey has the agents within $[0, 1]^2$. The agents in the predator-prey are randomly positioned within $[0, 1]^2$. The output layer of policy network of MADDPG for the environments provides the action as a five-sized tensor for hold, right, left, up, and down. We used 50,000 training episodes with 50 steps (total 2.5 million steps) for training the MARL model in the predator-prey. The experiments in this study were conducted based on the environments provided by <https://github.com/openai/multiagent-particle-envs>. All codes used in the experiments will be released.

Table 4: Hyper-parameters.

Hyper-parameter	Maze	Cooperative Navigation	Predator-Prey
Maximum timesteps		50	
N	1	2,3,4	
F		4	4
MADDPG Hyper-parameter			
# Policy network MLP units		(64, 64)	
# Q -network MLP units		(64, 64)	
network parameter initialization		Xavier uniform	
Nonlinear activation		ReLU	
Policy network learning rate		10^{-2}	
Q -network learning rate		10^{-2}	
τ for updating target networks		10^{-2}	
γ		0.95	
Replay buffer size		10^6	
Mini-batch size		1024	
Optimizer		Adam	
REMAX Hyper-parameter			
N_s		400	
F'		16	
σ		ReLU	
K	-	1	2
# VGAE decoder network MLP units		(32, 32)	
# surrogate model network MLP units		(64, 64)	
network parameter initialization		Xavier uniform	
Nonlinear activation		ReLU	
Training epochs		3	
Learning rate		10^{-4}	
λ		10^{-3}	
β		1	
Mini-batch size		1024	
Optimizer		Adam	
# Loops L for optimizing $f_\psi(z)$ w.r.t. z		400	
δ		10^{-1}	
η		$\mathcal{N}(0, \frac{1}{t})$	